Bright-green Upconversion Emission of Hexagonal LaF$_3$: Yb^{3+}, Er^{3+} Nanocrystals

Gejihu De, Weiping Qin,* Jisen Zhang, Dan Zhao, and Jishuang Zhang
*Key Laboratory of Excited State Processes, Changchun Institute of Optics, Fine Mechanics and Physics,
Chinese Academy of Science, Changchun 130033, P. R. China*

LaF$_3$: Yb^{3+}, Er^{3+} nanoparticles were synthesized through a simple hydrothermal method. The nanoparticles were well-crystallized and exhibited hexagonal structure with fine morphology, as indicated by powder X-ray diffraction, electron diffraction, and transmission electron microscopy. The nanocrystals present a bright-green upconversion luminescence under the 978-nm excitation of a laser diode, which provides a promising upconversion phosphor for optoelectronic or biological applications.

Fluorides doped with rare earth (RE) ions have been used in a wide range of applications such as lasers,[1] optical communications,[2] and display devices.[3] The tendency towards nanoscale science attracted the interest in nanosized optical functional materials. For fluorides, various nanostructures, such as nanotubes and nanowires, have been fabricated by hydrothermal method.[4,5] With the rapid shrinking in size in optical devices, nanometer-scale fluorides may play an essential role for their applications in high-density optical data storage, undersea communication, color displays, and infrared nanosensors in the near future. Recently, BaF$_2$: Nd nanoparticles (NPs) have been synthesized by a reverse microemulsion technique.[6] Er^{3+}, Nd^{3+}, and Ho^{3+}-doped LaF$_3$ NPs have also been prepared using capping agents, by which the obtained NPs are dispersible in organic solvents.[7] Furthermore, Heer et al. have reported the highly efficient multi-color upconversion (UC) emission in transparent colloids of lanthanide-doped NaYF$_4$ nanocrystals (NCs).[8] Meanwhile, RE-doped fluoride NCs have also been demonstrated to be a kind of promising UC fluorescence labels in biological detections.[9] The UC fluoride phosphors have been used to enhance the near-infrared response of silicon solar cell.[10] Nevertheless, in practical applications, some problems still arise from either the synthesis procedure or materials quality. The crystal structure and crystallization of the host turn out to affect the optical properties of luminescent centers. Thus, it is highly desirable to develop a method for fabricating monodisperse and well-crystallized fluoride NCs. In this letter, we report the preparation of Yb^{3+}–Er^{3+} codoped LaF$_3$ NCs and its green UC properties.

The LaF$_3$: Yb^{3+}, Er^{3+} NCs were synthesized by a simple hydrothermal method. In typical synthesis, cetyltrimethyl-ammonium chloride (CTAC, Aldrich) was selected as template. The rare earth solution were prepared by dissolving 0.95 mmol of La(NO$_3$)$_3$·6H$_2$O (Aldrich), 0.04 mmol of Yb(NO$_3$)$_3$·6H$_2$O (Aldrich) and 0.01 mmol of Er(NO$_3$)$_3$·6H$_2$O (Aldrich) into 12 mL of deionized water. Then 0.60 g of CTAC was completely dissolved into the rare earth solution to form clear mixture. The KF solution was obtained by dissolving 3 mmol of KF·2H$_2$O (Aldrich) into 4 mL of deionized water to provide F$^-$ ions. The KF solutions were added into the mixture under vigorous stirring to obtain the fluoride precursor. The suspension was stirred for additional 30 min before being transferred into a 25 mL

Teflon-lined autoclave. After the hydrothermal treatment at 120 °C (in air) for 12 h, the precipitate was then centrifuged, washed with absolute ethanol and distilled water several times, and then dried in a vacuum at room temperature. Finally, the powder was calcined at 400 °C for 30 min in an inert atmosphere.

The phase purity of the as-prepared products was evident with X-ray diffractometry (XRD) (model Rigaku RU-200b), using nickel-filtered Cu Kα radiation ($\lambda = 1.5406$ Å). The size and morphology were characterized by TEM (JEM, 2000EX 200 kV). The UC luminescence spectra were measured with a Hitachi F-4500 fluorescence spectrophotometer under the excitation by 978-nm light from a laser diode (LD, 2W).

Figure 1 presented the XRD pattern of the as-prepared sample. All the diffraction peaks can be readily indexed to the hexagonal LaF$_3$ phase (space group $P6_322$ (182)) with lattice constants $a = 0.716$, $c = 0.733$ nm, in good agreement with the standard values for the bulk hexagonal LaF$_3$ (JCPDS No. 72-1435). No impurity can be identified from the XRD pattern, suggesting that our synthesis was a promising method to prepare pure and single phased lanthanide fluorides.

The morphology of the final product was characterized by the TEM observation. As can be seen in the typical TEM images (Figure 2a), most of the particles dispersed on the copper grids show hexagonal morphology. The average edge length of the hexagon is about 15 nm. Figure 2b gives a magnified image of single LaF$_3$: Yb^{3+}, Er^{3+} NCs. Each nanocrystal exhibits good shape with hexagonal edges. The electron diffraction pattern

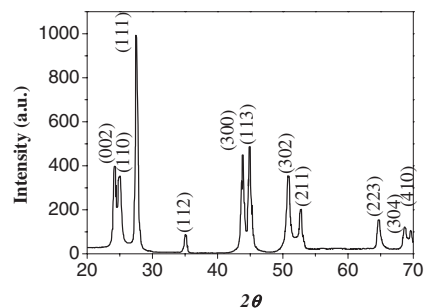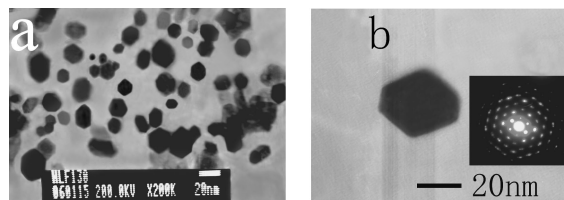**Figure 1.** XRD pattern of hexagonal NCs LaF$_3$: Yb^{3+}, Er^{3+}.

Figure 2. (a) TEM image of hexagonal NCs LaF$_3$: Yb^{3+}, Er^{3+}. (b) TEM image of an individual LaF$_3$: Yb^{3+}, Er^{3+} NCs. Inset: electron diffraction patterns of the NCs.

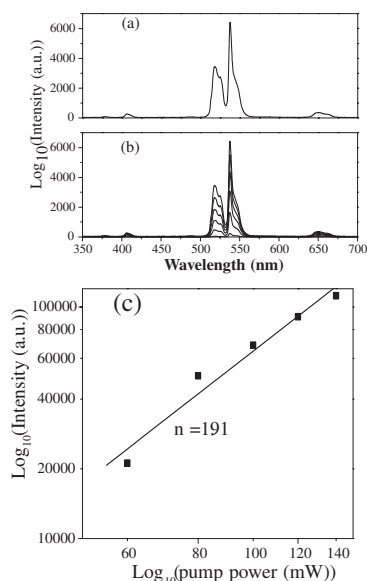**Figure 3.** (a) Room-temperature UC emission spectra of hexagonal NCs LaF$_3$: Yb^{3+}, Er^{3+}. (b) UC spectra of the LaF$_3$: Yb^{3+}, Er^{3+} NCs under the 978-nm excitation with different powers (40–140 mW). (c) The dependence of the UC luminescence intensity on the pump power for the green emissions.

Figure 4. Schematic diagram of Yb^{3+}-sensitized Er^{3+} upconversion in LaF$_3$: Yb^{3+}, Er^{3+} hexagonal NCs under 978-nm excitation.

taken from individual NCs (inset of Figure 2b) clearly indicates the crystalline nature, and confirms further that the NCs have hexagonal symmetry.

Yb^{3+}–Er^{3+}-codoped fluorides were efficient material systems for near-infrared to visible frequency UC, as demonstrated elsewhere.[11] For the LaF$_3$: Yb^{3+}, Er^{3+} NCs, bright-green luminescence can be clearly observed with naked eyes when the sample was excited by a 978-nm diode laser with excitation power of 140 mW. This suggests that the NCs were promising UC nanophosphors. Figure 3a presents the room-temperature UC emission spectrum of the LaF$_3$: Yb^{3+}, Er^{3+} NCs. The four emission peaks in the spectrum correspond to the following transitions $^2H_{9/2} \rightarrow {}^4I_{15/2}$ ($\approx$408 nm), $^2H_{11/2} \rightarrow {}^4I_{15/2}$ ($\approx$518 nm), $^4S_{3/2} \rightarrow {}^4I_{15/2}$ ($\approx$538 nm), $^4F_{9/2} \rightarrow H_{15/2}$ ($\approx$650 nm), respectively. Here we focus our discussion on the green emissions, which was dominant in the UC luminescence for the LaF$_3$: Yb^{3+}, Er^{3+} NCs. Figure 3b show the UC luminescence spectra of the 15 nm LaF$_3$: Yb^{3+}, Er^{3+} NCs at different excitation powers. The red emissions of $^4F_{9/2} \rightarrow {}^4I_{15/2}$, green emissions of $^4S_{3/2}$, $^2H_{11/2} \rightarrow {}^4I_{15/2}$ and blue emission $^2H_{9/2} \rightarrow {}^4I_{15/2}$ were observed. It is obvious that the relative intensity of the green emission increased with the excitation power. Figure 3c shows log–log plot of the emission intensity of the 15 nm LaF$_3$: Yb^{3+}, Er^{3+} powders as a function of excitation power. For unsaturated UC, emission intensity, I_{em}, is proportional to $I_{ex}{}^n$, where I_{ex} is the intensity of the excitation light and the integer n is the number of photons involved in the UC process. The value of $n = 1.91$ was obtained by fitting the intensity dependence of the 518-nm and 538-nm emissions, confirming two-photon processes are responsible for the green UC.

In Yb^{3+}–Er^{3+}-codoped systems, different processes may result in UC. These processes include multistep excited state absorption (ESA), energy transfer (ET) between neighboring Er^{3+} ions and "Addition de Photons par Transfert d'Energie"
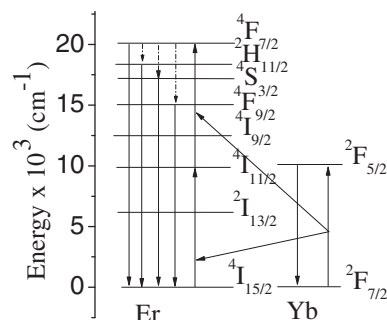
(APTE) between Yb^{3+} and Er^{3+}. Among these processes, APTE is the most efficient. Infrared to green ($^2H_{11/2}$, $^4S_{3/2} \rightarrow {}^4I_{15/2}$ transitions) and to red ($^4F_{9/2} \rightarrow {}^4I_{15/2}$ transition) upconverted emissions in Yb^{3+}–Er^{3+}-codoped systems have been widely investigated. Figure 4 shows the energy levels and UC mechanism in Yb^{3+}–Er^{3+}-codoped system. As indicated by the arrows, Yb^{3+} ion was excited from the ground state $^2F_{7/2}$ to the excited state $^2F_{5/2}$ by an infrared (978 nm) photon. The Yb^{3+} ion may transfer the energy to the Er^{3+} ion, which can promote an electron from $^4I_{15/2}$ to $^4I_{11/2}$ state, and if the latter is already populated, the electron may transit from the $^4I_{11/2}$ to the $^4F_{7/2}$ states. Subsequently, nonradiative relaxations could populate the $^2H_{11/2}$ and $^4S_{3/2}$ states, which was the emitting levels for the green luminescence. As it seen, the green UC luminescence is due to two-photon processes.

In summary, Yb^{3+}–Er^{3+}-codoped LaF$_3$ NCs were synthesized by hydrothermal method. XRD analysis showed that the products were single hexagonal phase. TEM showed that the products have uniform grain shapes and almost equiaxed with an average size of 15 nm. The efficient UC emission of LaF$_3$: Yb^{3+}, Er^{3+} NCs, emitting in the red, green, and ultraviolet regions, at room temperature. Excitation of the samples with 978 nm populates the $^4F_{7/2}$ state via two successive energy transfer from the Yb^{3+} ions and yields intense green UC luminescence.

References
1   R. Reisfeld and C. K. Jorgensen, "Lasers and Excited States of Rare Earths," Springer, Berlin (1977).
2   P. C. Becker, N. A. Olsson, and J. R. Simpson, "Erbium doped Amplifiers: Fundamentals and Technology," Academic Press, San Diego (1999).
3   G. Blasse and B. C. Grabmaier, "Luminescent Materials," Springer, Berlin (1994).
4   L. F. Liang, H. F. Xu, Q. Su, H. Konishi, Y. B. Jiang, M. M. Wu, Y. F. Wang, and D. Y. Xia, *Inorg. Chem.*, **43**, 1594 (2004).
5   M. H. Cao, C. W. Hu, and E. B. Wang, *J. Am. Chem. Soc.*, **125**, 11196 (2003).
6   C. M. Bender and J. M. Burlitch, *Chem. Mater.*, **12**, 1969 (2000).
7   J. W. Stouwdam and F. C. J. M. van Veggel, *Nano Lett.*, **2**, 733 (2002).
8   S. Heer, K. Kömpe, H.-U. Güdel, and M. Haase, *Adv. Mater.*, **16**, 2102 (2004).
9   G. Yi, H. Lu, S. Zhao, Y. Ge, W. Yang, D. Chen, and L.-H. Guo, *Nano Lett.*, **4**, 2191 (2004).
10 A. Shalav, B. S. Richards, and T. Trupke, *Appl. Phys. Lett.*, **86**, 013505-1 (2005).
11 G. Qin, W. Qin, S. Huang, C. Wu, B. Chen, S. Lu, and E. Shulin, *Solid State Commun.*, **120**, 211 (2001).